



Title	Methanol-Triggered Turn-On-Type Photoluminescence in L-Cysteinato Palladium(II) and Platinum(II) Complexes Supported by a Bis-Diphenylphosphine Ligand
Author(s)	Shimizu, Tsutomu; Yoshinari, Nobuto; Nozaki, Koichi et al.
Citation	Inorganic Chemistry. 2016, 55(5), p. 2030-2036
Version Type	AM
URL	https://hdl.handle.net/11094/57156
rights	© 2016 American Chemical Society
Note	

The University of Osaka Institutional Knowledge Archive : OUKA

<https://ir.library.osaka-u.ac.jp/>

The University of Osaka

Methanol-Triggered Turn-On-Type Photoluminescence in L-Cysteinato Palladium(II) and Platinum(II) Complexes Supported by a Bis- Diphenylphosphine Ligand

Nobuto Yoshinari,[†] Tsutomu Shimizu,[†] Koichi Nozaki,[‡] Takumi Konno^{,†}*

[†]Department of Chemistry, Graduate School of Science, Osaka University, Toyonaka, Osaka
560-0043, Japan.

[‡]Graduate School of Science and Engineering, University of Toyama, 3190 Gofuku, Toyama
930-8555, Japan.

*konno@chem.sci.osaka-u.ac.jp

ABSTRACT: The selective detection of methanol by photoluminescence under environmental conditions has been a great challenge for materials science. Herein, a reversible, turn-on-type photoluminescence triggered by methanol vapor in square-planar palladium(II) and platinum(II) complexes, newly prepared from $[MCl_2(dppp)]$ and L-cysteine, is reported. Both the ‘turn-on’ and ‘turn-off’ states of the complexes were crystallographically characterized, which revealed the presence of intermolecular $OH\cdots O$ and $CH\cdots\pi$ interactions between methanol and the complex molecules in the ‘turn-on’ state. These interactions prevent the vibrational quenching of the luminescence, leading to the turn-on-type luminescence in this system.

INTRODUCTION

Luminescent coordination compounds have attracted considerable attention because of their potential availability as chemical sensors to detect volatile organic compounds (VOCs) in a manner visible to the naked eye in working environments.¹ Among VOCs, methanol is particularly important for detection because it is readily metabolized to highly toxic formaldehyde and formic acid in the human body.² Thus, a number of luminescent metal complexes that can detect methanol vapor have recently been developed.³⁻⁹ However, almost all of the methanol detection compounds show a luminescence energy shift (color change)³⁻⁷ or luminescence quenching (turn-off),^{8,9} which are inferior to the luminescence enhancement from darkness (turn-on) in terms of eye visibility. In addition, the compounds often respond to various VOCs in addition to methanol.³⁻⁹ Thus, selective, turn-on-type luminescence triggered by methanol vapor under environmental conditions has rarely been achieved by coordination compounds.¹⁰

As part of our ongoing study on the coordination behavior of a hydrophilic sulfur-containing amino acid in the presence of a hydrophobic coligand,¹¹⁻¹³ we synthesized simple, mononuclear

palladium(II) and platinum(II) complexes with mixed 1,3-bis(diphenylphosphino)propane (dppp) and L-cysteinate (L-cys), $[M(dppp)(L-cys)]$ ($M = Pd^{II}, Pt^{II}$). Whereas these complexes are not emissive in the hydrate form, strong yellow emission is observed in the presence of methanol molecules of crystallization. Remarkably, the non-emissive hydrate form and the emissive methanolic form are reversibly converted to each other by exposure to methanol vapor and by standing in an ambient atmosphere (Figure 1). Herein, we report on the preparation and structural characterization of both the non-emissive and emissive forms of these complexes, together with their emission properties. As far as we know, these are the first examples of reversible, turn-on-type photoluminescent compounds that sense methanol vapor.

RESULTS AND DISCUSSION

Synthesis and characterization of [1]. The 1:1:2 reaction of $[PtCl_2(dppp)]$,¹⁴ L-H₂cys, and KOH in methanol/water (3:1) gave a colorless solution, from which colorless needle crystals (**1a**) were obtained in a high yield. The ESI mass spectrum of **1a** in methanol showed a dominant signal centered at $m/z = 727.1$, which corresponds to a protonated form of the platinum(II) complex with mixed dppp and L-cys, $[Pt(dppp)(L-cys)]$ ([1]). In the ¹H NMR spectrum in DMSO-*d*₆, a freshly prepared sample of **1a** showed a signal due to methanol at δ 3.17, in addition to a single set of signals due to [1] (Figure S1),¹⁵ indicative of the presence of methanol molecules of crystallization in **1a**.

The structure of **1a** was determined by single-crystal X-ray crystallography. The asymmetric unit of **1a** contains two crystallographically independent, yet essentially the same, complex molecules and three water and three methanol molecules. Each complex molecule has a square-planar mononuclear structure in [1], coordinated by *N,S*-chelating L-cys and *P,P*-chelating dppp

ligands (Figure 2a). The Pt–N and Pt–S distances (av. Pt–N = 2.13 Å, Pt–S = 2.33 Å) and the N–Pt–S angle (av. 85.2°) in **[1]** are similar to those in *cis*-[Pt(D-pen)₂]²⁻.¹⁶ The Pt–P distance (av. 2.28 Å) trans to the S atom is slightly longer than that (av. 2.24 Å) trans to the N atom because of the stronger trans influence due to the S atom. The carboxylate group in **[1]** does not participate in the coordination and exists in the deprotonated form, consistent with its IR spectrum, which shows a C=O stretching band at 1603 cm⁻¹ (Figure S2).^{15,17} The five-membered *N,S*-chelate ring in **[1]** adopts a δ gauche conformation such that the carboxylate group has an axial orientation, whereas the six-membered *P,P*-chelate ring has a chair conformation.

Luminescence behavior of [1]. At ambient temperature, freshly prepared needle crystals of **1a** (**[1]**·1.5MeOH·1.5H₂O) showed an intense yellow emission with a quantum yield of 10% in the solid state. The maximal wavelengths of the emission and the excitation spectra of **1a** are 531 nm (18.8×10^3 cm⁻¹) and 348 nm (23.7×10^3 cm⁻¹), respectively (Figure 3b). The large Stokes shift (4.9×10^3 cm⁻¹), together with the long emission lifetime of a microsecond order ($\tau = 1.11$ μ s), is indicative of the phosphorescent character of its emission.¹⁸ The density functional theory (DFT) calculations revealed that the highest occupied molecular orbital (HOMO) is dominantly composed of p(S) and d(Pt) orbitals, while the lowest unoccupied molecular orbital (LUMO) is comprised of the $\pi^*(\text{dppp})$ orbital. Thus, the phosphorescence can be assigned as arising from a triplet MLL'CT (Pt-S \rightarrow phosphine) transition.

When **1a** was placed in air at ambient temperature, its yellow emission gradually decreased and completely disappeared within several hours (Figure 3c). The elemental analytical data of this non-emissive, colorless, crystalline sample (**1b**) were consistent with a hydrate form of **[1]**.¹⁹ In addition, the ¹H NMR spectrum of **1b** in DMSO-*d*₆ was identical with that of **1a**, except for the lack of signals due to methanol (Figure S1).¹⁵ Thus, methanol molecules of crystallization are

released from **1a** in air with the concomitant incorporation of water molecules, giving the non-emissive sample **1b**.²⁰ The powder X-ray diffraction (PXRD) pattern for **1b** is different from that for **1a** (Figure S3),¹⁵ indicative of the difference in the crystal packing structures between **1a** and **1b**. The reverse conversion from **1b** to **1a** was also investigated. When **1b** was exposed to methanol vapor, the intense yellow luminescence was recovered within 1 minute (Figure 3d). In addition, the PXRD pattern of the recovered sample was superimposable with that of **1a**, which indicates reversible crystal-to-crystal conversion between **1a** and **1b** (Figure S3).¹⁵ The on-off luminescence switching was repeatable for at least 5 cycles (Figure 3e).

To check whether a similar reversible conversion is induced by other volatile organic compounds (VOCs), a solid sample of **1b** was exposed to several common VOCs, including acetone, CHCl₃, CH₂Cl₂, C₂H₅OH, CH₃CN, THF, toluene, benzene, cyclohexane, and CH₃NH₂. However, no emission was observed after exposure of these VOCs to **1b** (Figure S4).^{15,21} The ¹H NMR spectroscopy showed that these VOCs were not incorporated in a solid sample of **1b**, indicating that this compound is a turn-on-type luminescence sensor that is highly selective toward methanol vapor.

The structural characterization of the non-emissive **1b** by single-crystal X-ray crystallography, together with that of the emissive **1a**, is required to clarify the mechanism of this switchable, selective, turn-on-type luminescence phenomenon. Initial attempts to determine the structure of the needle crystals of **1b**, which were obtained by allowing crystals of **1a** to stand in air, were unsuccessful because of the poor crystal quality. However, X-ray quality crystals of **1b** were produced from non-emissive block crystals of **1c** ([**1**]·7H₂O), which were obtained by recrystallizing **1a** from methanol/water (1:3), that is, standing crystals of **1c** in air at room

temperature for 1 day gave non-emissive block crystals of **1b**, the PXRD pattern of which is matched well with that of **1b** derived from **1a**. (Figure S5).¹⁵

X-ray analysis demonstrated that both **1b** and **1c** contain complex molecules of [**1**] and several solvated water molecules in the asymmetric unit. No significant difference in the molecular structure of [**1**] is observed between **1a**, **1b**, and **1c** (Figures 4a and 4c), but the packing motifs of the complex molecules in the crystals are quite different. In the emissive **1a**, an amine group of [**1**] forms a strong intermolecular hydrogen bond with a carboxylate group of a neighboring complex molecule ($N\cdots O = 2.66 \text{ \AA}$), constructing a four-fold helix structure with left-handedness (Figures 2b and 2c). In **1a**, methanol molecules of crystallization exist in the void space and are connected to carboxylate groups through $O-H\cdots O$ hydrogen bonds (2.72 \AA). Moreover, each methanol molecule forms a $C-H\cdots\pi$ interaction with two dppp phenyl groups from two different complex molecules (av. 3.9 \AA) (Figure 2d). In the non-emissive **1b** and **1c**, an amine group forms a weak intermolecular hydrogen bond with a carboxylate group of an adjacent complex molecule ($N\cdots O = 2.97 \text{ \AA}$ for **1b** and 2.93 \AA for **1c**), affording dimeric and tetrameric structures, respectively (Figures 4b and 4d). However, no clear interactions exist between the guest water molecules and dppp ligands in **1b** and **1c**. It is assumed that the co-existence of $N-H\cdots O$ and $C-H\cdots\pi$ interactions in **1a**, which effectively prevent the emission quenching by molecular vibration, is responsible for the strong emission of **1a** at ambient temperature.^{22,23} Whereas several examples of vapor-induced turn-on-type photoluminescent compounds have been reported, they commonly involve only a single type of non-covalent interaction, such as coordination, hydrogen-bonding, or $\pi\cdots\pi$ interactions, between the guest and host molecules.²⁴⁻²⁶

Synthesis and characterization of [2]. Prompted by the unique emission properties found for [1], we also synthesized the corresponding palladium(II) complex, [Pd(dppp)(L-cys)] ([2]). This complex was initially isolated as yellow needle crystals that contained both methanol and water molecules of crystallization, [2]·1.5MeOH·1.5H₂O (**2a**), from the reaction solution of [PdCl₂(dppp)]²⁷ with L-cys in methanol/water (3:1). Two other types of crystals containing only water molecules of crystallization, [2]·4H₂O (**2b**) and [2]·7H₂O (**2c**), were prepared by the same procedures used for **1b** and **1c**.

The structures of **2a**, **2b**, and **2c** were established by single-crystal X-ray crystallography, which revealed that **2a**, **2b**, and **2c** are isostructural with **1a**, **1b**, and **1c**, respectively (Figures S6-S8).¹⁵ Crystals of **2a** exhibited an orange emission at 635 nm with a quantum yield of 1.7% at room temperature (Figure S9).¹⁵ The DFT calculation study showed that the HOMO of **2a** is dominated by p(S) orbital and its LUMO is composed of $\pi^*(\text{dppp})$ and d(Pd) orbitals, implying that the emission of **2a** is assignable as a triplet LML'CT (S to Pd-phosphine) transition. This emission origin is different from the origin assigned for **1a** (MLL'CT). It is considered that the lower energy of the $d_{x^2-y^2}$ orbital of Pd^{II} relative to that of Pt^{II} due to the smaller ligand-field splitting stabilizes the LUMO of **2a** to decrease its emission energy. As in the case of **1a**, the orange emission for **2a** gradually disappeared in air and was quickly recovered after exposure to methanol vapor (Figure S10), accompanied by structural conversion between **2a** and **2b**.¹⁵ Eye-detectable emission at ambient temperature for palladium(II) compounds is relatively rare and is limited for those containing porphyrin or cyclometalate ligands^{28,29} because of the lower energy of metal-centered excited state(s), which results in a facile non-radiation deactivation *via* molecular distortion.²⁸ To our knowledge, the on/off-switching of emission for palladium(II) compounds in response to outer factors has not been reported.

EXPERIMENTAL SECTION

Caution! Methanol is volatile, flammable, and poisonous.

Preparation of [Pt(dppp)(L-cys)]·1.5H₂O·1.5MeOH (**1a**) and [Pt(dppp)(L-cys)]·4H₂O (**1b**).

To a white suspension of [PtCl₂(dppp)] (500 mg, 0.74 mmol) in methanol (30 mL) was added a colorless solution containing L-H₂cys (91 mg, 0.75 mmol) in 1.0 M aqueous KOH (1.5 mL, 1.5 mmol). The mixture was stirred at room temperature for 4 h, which afforded a colorless solution. To the solution was added water (10 mL), followed by allowing to stand at room temperature for 4 d. The resulting colorless needle crystals of **1a** suitable for X-ray analysis were collected by filtration. When the colorless needle crystals of **1a** were allowed to stand in air for 1 day, they are effloresced to give a white crystalline powder of **1b**. Yield: 394 mg (68%). Anal. Calcd for [**1**]·3H₂O = C₃₀H₃₇NO₅P₂PtS: C, 46.15; H, 4.78; N, 1.79%. Found: C, 46.47; H, 4.53; N, 1.86%. ESI-MS (CH₃OH, m/z): 727.1 (M+H)⁺. ¹H NMR (CD₃OD, ppm from TMS): 1.92-2.33 (2H, m, CH₂), 2.80-3.03 (6H, m, CH₂), 3.44-3.64 (1H, m, CH), 7.32-7.73 (20H, m, Ph). ³¹P NMR (CD₃OD, ppm from 80% H₃PO₄): -9.42 (t, J_{Pt} = 1591 Hz), -4.21 (t, J_{Pt} = 1252 Hz). Electronic absorption spectrum in CH₃OH [ν , 10³ cm⁻¹ (log ϵ , M⁻¹ cm⁻¹): 29.85 (2.39 sh), 34.79 (3.46), 40.92 (4.37), 45.25 (4.63). CD spectrum in CH₃OH [ν , 10³ cm⁻¹ ($\Delta\epsilon$, M⁻¹ cm⁻¹): 29.05 (+0.175), 33.83 (-0.15), 38.82 (-0.146).

Preparation of [Pt(dppp)(L-cys)]·7H₂O (1c**) and conversion of **1c** to **1b**.** The colourless block crystals of [**1**]·7H₂O (**1c**) suitable for X-ray analysis were obtained by recrystallization of **1a** from H₂O/CH₃OH (v/v = 3:1). Anal. Calcd for [**1**]·7H₂O = C₃₀H₄₅NO₉P₂PtS: C, 42.25; H, 5.32; N, 1.64%. Found: C, 42.37; H, 5.63; N, 1.66%. When the resulting block single-crystals of **1c** were allowed to stand in air at room temperature for 1 day, they were converted to single-

crystals of **1b**, which were also suitable for X-ray analysis, through a single-crystal to single-crystal transformation process.

Preparation of [Pd(dppp)(L-cys)]·1.5H₂O·1.5MeOH (2a) and [Pd(dppp)(L-cys)]·4H₂O (2b). To a pale pink suspension of [PdCl₂(dppp)] (500 mg, 0.85 mmol) in methanol (30 mL) was added a colorless solution containing L-H₂cys (104 mg, 0.86 mmol) in 1.0 M aqueous KOH (1.9 mL, 1.9 mmol). The mixture was stirred at room temperature for 2 h, which afforded a yellow solution. To the solution was added water (10 mL), followed by allowing to stand at room temperature for 4 d. The resulting yellow needle crystals of **2a** suitable for X-ray analysis were collected by filtration. When the yellow needle crystals of **2a** were allowed to stand in air for 1 day, they are effloresced to give a yellow crystalline powder of **2b**. Yield: 388 mg (66%). Anal. Calcd for [**2**]·3H₂O = C₃₀H₃₇NO₅P₂PdS: C, 52.07; H, 5.39; N, 2.02%. Found: C, 52.16; H, 5.31; N, 2.08%. ESI-MS (CH₃OH, m/z): 638.1 (M+H)⁺. ¹H NMR (CD₃OD, ppm from TMS): 1.97-2.24 (2H, m, CH₂), 2.67-2.97 (6H, m, CH₂), 3.65-3.69 (1H, m, CH), 7.33-7.71 (20H, m, Ph). ³¹P NMR (CD₃OD, ppm from 80% H₃PO₄): -1.21 (s), 11.40 (s). Electronic absorption spectrum in CH₃OH [ν , 10³ cm⁻¹ (log ϵ , M⁻¹ cm⁻¹): 24.62 (2.17 sh), 34.25 (4.16), 39.28 (4.31), 44.76 (4.73). CD spectrum in CH₃OH [ν , 10³ cm⁻¹ ($\Delta\epsilon$, M⁻¹ cm⁻¹): 24.39 (+0.216), 34.72 (-2.30), 39.6 (-2.49), 43.9 (-1.09).

Preparation of [Pd(dppp)(L-cys)]·7H₂O (2c) and conversion to 2b. The yellow block crystals of [**2**]·7H₂O (**2c**) suitable for X-ray analysis were obtained by recrystallization of **2a** from H₂O/CH₃OH (v/v = 3:1). When the resulting block single-crystals of **2c** were allowed to stand in air at room temperature for 1 day, they were converted to single-crystals of **2b**, which

were also suitable for X-ray analysis, through a single-crystal to single-crystal transformation process.

Vapour Diffusion of Volatile Organic Compounds (VOCs) for 1b and 2b.

Vapour diffusion experiments were carried out using air saturated with various VOCs.

Physical measurements. The elemental analyses (C, H, N) were performed at Osaka University using Yanaco CHN coda MT-5 or MT-6. The IR spectra were recorded on a JASCO FT/IR-4100 infrared spectrometer using KBr disks at room temperature. The ^1H and ^{31}P NMR spectra were recorded with a JEOL GSX400 (400 MHz) or a JEOL ECA500 (500 MHz) spectrometers at 25 °C using tetramethylsilane (TMS, δ 0.00 ppm) as the internal standard for ^1H , triphenylphosphate (δ -17.60 ppm) as the external standard for ^{31}P . The NMR data were illustrated as Figures S11 and S12.¹⁵ The electronic absorption spectra were recorded with a JASCO V-660 spectrophotometer at room temperature. The diffuse reflection spectra were measured with a JASCO V-670 UV/Vis/NIR spectrometer. The circular dichroism (CD) spectra were recorded with a JASCO J-820 spectropolarimeter at room temperature. Electrospray ionization (ESI) mass spectra were recorded on a QSTAR Elite LC-MS/MS System in CH_3OH .

Luminescence measurements. The luminescence spectra were recorded on a JASCO FP-8500 spectrometer at room temperature in the solid state. The emission quantum yields (Φ) were measured with a lab-made absolute emission quantum yield measuring system using an integrating sphere (6 in., Labsphere Inc.), the internal surface of which was coated with highly reflective Spectralon. A sample powder in a flat quartz cell (10 mm diameter, 1 mm height) placed at the bottom of the integrating sphere was excited with a monochromated light (355–365 nm) introduced from the top of the integrating sphere through a liquid light guide (deep UV

model, Newport Co.). The emission from a detection exit of the integrating sphere was focused into a grating spectrometer (Triax 1900, Jobin Yvon) equipped with a CCD image sensor (S7031, Hamamatsu). The absolute quantum yield of emission was calculated according to the method described in the literature.³⁰ The emission lifetimes were determined using the measuring system previously reported.³¹ The sample was photoexcited using the third harmonic of a Q-switched Nd³⁺:YAG laser (Continuum Surelite I-10, λ 355 nm). The observed decay profile of the emission intensity was fit to two or three exponential functions with convolution of the instrumental response function of the measuring system. The data were summarized as Table 1.

Powder X-ray diffraction measurements. High quality powder X-ray diffraction pattern were recorded for **1a**, **1b** prepared from **1a**, **1c**, **2a**, **2b** prepared from **2a**, and **2c** at room temperature, in transmission mode [synchrotron radiation $\lambda = 1.000 \text{ \AA}$; 2θ range = $0\text{--}78^\circ$; step width = 0.01° ; data collection time = 3 min] on a diffractometer equipped with a white imaging plate detector at SPring-8 BL02B2 beamline. The crystals were put into 0.3 mm glass capillary tubes. The samples were rotated during the measurements. The diffraction patterns were collected with a large Debye–Scherrer camera. The powder simulation patterns were generated from the single-crystal X-ray structures using Mercury 3.0, and corrected for thermal expansion. The synchrotron radiation experiments were performed at the BL02B2 of SPring-8 with the approval of the Japan Synchrotron Radiation Research Institute (JASRI) (Proposal No. 2015A1506 and 2015A1520). The high quality powder X-ray diffraction patterns were illustrated in Figures S13 and S14.¹⁵ Other powder X-ray diffraction measurement experiments were performed on a RIGAKU RINT2000 in reflection mode [CuK α ($\lambda = 1.5418 \text{ \AA}$); 2θ range = $0\text{--}30^\circ$; step width = 0.02° ; data collection time = 15 min].

X-ray Structural Determinations. The single crystal X-ray diffraction measurements for crystals **1a**, **1b**, **1c**, **2a**, **2b**, and **2c** were performed on a Rigaku R-AXIS VII imaging plate and Vari-Max with graphite monochromated Mo-K α radiation ($\lambda = 0.71075$ Å). The intensity data were collected by the ω -scan technique and empirically corrected for absorption. The structures of complexes were solved by direct methods using SHELXS-97.³² The structure refinements were carried out using full matrix least-squares using SHELXL-2014.³² Several unusual diffractions were omitted by OMIT commands so as to improve data quality. The crystal data were summarized in Table 2.

For **1a**, hydrogen atoms were placed at calculated positions, except those of water molecules, and were calculated using riding models. All non-hydrogen atoms except for those of several water molecules were refined anisotropically. For **1c** and **2c**, several DFIX restraints were used in order to avoid unusual contact among water molecules. Hydrogen atoms were placed at calculated positions, except those of water molecules, and were calculated using riding models. All non-hydrogen atoms except for those of several water molecules were refined anisotropically. For **1b**, **2a**, and **2b**, hydrogen atoms were placed at calculated positions, except those of water molecules, and were calculated using riding models. All non-hydrogen atoms were refined anisotropically.

DFT calculations. To elucidate the origin of emission bands observed for **1a** and **2a**, molecular orbital (MO) calculations were performed using the Gaussian 09 program³³ at the B3LYP³⁴ level using a Lanl2DZ³⁵ basis set. The single-point and time-dependent DFT calculations were carried out for [Pt(dppp)(L-cys)] (**[1]**) and [Pd(dppp)(L-cys)] (**[2]**). The structural parameters were taken from the single-crystal X-ray structures of **1a** and **2a**. The components of the MOs are listed in Tables S1 and S3.¹⁵ The contour plots of selected MOs near

frontier orbitals are demonstrated in Figures S15 and S16.¹⁵ The results of Mulliken population analysis of MOs near frontier orbitals, as well as TD-DFT calculations, are summarized in Tables S2 and S4.¹⁵

For [1], the LUMO is dominated by dppp (81%) orbitals, and the HOMO possesses large contributions from sulfur 3p (72%) and platinum 5d (17%) orbitals. TD-DFT calculations indicated that the lowest-energy transition occurs centered at 361 nm, which involves several one-electron transitions from the HOMO to the LUMO and LUMO + 2. This result is consistent with the appearance of an intense absorption band at 331 nm for [1], and thus the origin of this band is assignable as arising from Pt(5d)-S(3p) to dppp(π^*), which can be interpreted as the metal(platinum)-ligand(thiolate) to ligand(phosphine) charge transfer (MLL'CT) transition.

For [2], the LUMO is possesses large contributions from dppp (45%) and palladium 4d (29%) orbitals, and the HOMO has large contributions from sulfur 3p (75%) orbitals. TD-DFT calculations indicated that the lowest-energy transition occurs centered at 444 nm, which involves several one-electron transitions from the HOMO to the LUMO. This result is consistent with the appearance of an intense absorption band at 418 nm for [2], and thus the origin of this band is assignable as arising from S(3p) to Pd(4d)-dppp(π^*), which can be interpreted as the ligand(thiolate) to metal(palladium)-ligand(phosphine) charge transfer (LML'CT) transition.

CONCLUDING REMARKS

In this study, we created a simple but functional square-planar coordination system of platinum (II) that shows an on-off switch with yellow emission. The switch of emission was selectively turned on by methanol vapor and automatically turned off under environmental conditions. The same result was achieved for the corresponding palladium(II) system, which

shows an on-off switch with orange emission. X-ray quality single-crystals for both the ‘turn-on’ and ‘turn-off’ states of the platinum(II) and palladium(II) complexes were successfully prepared, which revealed the importance of O–H \cdots O and C–H \cdots π interactions between the host complex molecules and the guest methanol molecules for the appearance of photoluminescence. This study shows that the introduction of both hydrophilic and hydrophobic moieties in a luminophore is a promising way to create sensing materials that are highly selective toward small volatile molecules under ambient conditions.

ASSOCIATED CONTENT

Supporting Information. X-ray crystallographic files in CIF format for the structures in this work, ^1H and ^{31}P NMR spectra (Figures S1, S11, and S12), IR spectra (Figure S2), PXRD patterns (Figures S3, S5, S13, S14, and S18), emission spectra (Figures S4, S9, and S10), the results of DFT calculations (Table S1-S4, Figures S15 and S16), and TG analysis plots (Figure S17). This material is available free of charge via the Internet at <http://pubs.acs.org>.

AUTHOR INFORMATION

Corresponding Author

*E-mail: konno@chem.sci.osaka-u.ac.jp.

Notes

The authors declare no competing financial interests.

ACKNOWLEDGMENT

This work was supported by JST, CREST and JSPS KAKENHI Grant Numbers 15K21127, 25870387, 25600005, and 25410064.

REFERENCES

- (1) (a) Zhao, Q.; Li, F.; Huang, C. *Chem. Soc. Rev.* **2010**, *39*, 3007-3030. (b) Zhang, X.; Li, B.; Chen, Z.-H.; Chen, Z.-N. *J. Mater. Chem.* **2012**, *22*, 11427-11441. (c) Wenger, O. S. *Chem. Rev.* **2013**, *113*, 3686-3733. (d) Kobayashi, A.; Kato, M. *Eur. J. Inorg. Chem.* **2014**, 4469-4483.
- (2) Kruse, J. A. *Intensive Care Med.* **1992**, *18*, 391-397.
- (3) (a) Lu, W.; Chan, M. C. W.; Cheung, K.-K.; Che, C.-M. *Organometallics*, **2001**, *20*, 2477-2486. (b) Wadas, T. J.; Wang, Q.-M.; Kim, Y.-J.; Flaschenreim, C.; Blanton, T. N.; Eisenberg, R. *J. Am. Chem. Soc.* **2004**, *126*, 16841-16849. (c) Grove, L. J.; Rennekamp, J. M.; Jude, H.; Connick, W. B. *J. Am. Chem. Soc.* **2004**, *126*, 1594-1595. (d) Pattacini, R.; Giansante, C.; Ceroni, P.; Maestri, M.; Braunstein, P. *Chem. Eur. J.* **2007**, *13*, 10117-10128. (e) Forniés, J.; Fuertes, S.; Lopez, J. A.; Martin, A.; Sicilia, V. *Inorg. Chem.* **2008**, *47*, 7166-7176. (f) Du, P. *Inorg. Chim. Acta* **2010**, *363*, 1355-1358.
- (4) Abe, T.; Suzuki, T.; Shinozaki, K. *Inorg. Chem.* **2010**, *49*, 1794-1800.
- (5) Mizukami, S.; Houjou, H.; Sugaya, K.; Koyama, E.; Tokuhisa, H.; Sasaki, T.; Kanetsato, M. *Chem. Mater.* **2005**, *17*, 50-56.
- (6) Osawa, M.; Kawata, I.; Igawa, S.; Hoshino, M.; Fukunaga, T.; Hashizume, D. *Chem. Eur. J.* **2010**, *16*, 12114-12126.
- (7) Li, Y.-J.; Deng, Z.-Y.; Xu, X.-F.; Wu, H.-B.; Cao, Z.-X.; Wan, Q.-M. *Chem. Commun.* **2011**, *47*, 9179-9181.
- (8) Hudson, Z. M.; Sun, C.; Harris, K. J.; Lucier, B. E. G.; Schurko, R. W.; Wang, S. N. *Inorg. Chem.* **2011**, *50*, 3447-3457.

(9) Wang, H.-M.; Liu, H.-P.; Chu, T.-S.; Yang, Y.-Y.; Hu, Y.-S.; Liu, W.-T.; Ng, S. W. *RSC Adv.* **2014**, *4*, 14035-14041.

(10) Zhu and coworkers have recently reported a Zn-based MOF that shows the selective, sensitive, turn-on type methanol detection in an alcoholic solution. However, the system is not applicable for the detection of methanol vapor because the MOF framework collapses once the guest water molecules are removed. See: Jin, Z.; He, H.; Zhao, H.; Borjigin, T.; Sun, F.; Zhang, D.; Zhu, G. *Dalton Trans.* **2013**, *42*, 13335-13338.

(11) (a) Igashira-Kamiyama, A.; Fukushima, A.; Konno, T. *Chem. Eur. J.* **2013**, *19*, 16532-16536. (b) Kuwamura, N.; Hayashida, K.; Tsuge, K.; Yoshinari, N.; Konno, T. *Chem. Lett.* **2014**, *43*, 1846-1848. (c) Yokoi, A.; Yoshinari, N.; Konno, T. *J. Incl. Phenom. Macrocycl. Chem.* **2015**, *82*, 123-133.

(12) (a) Hashimoto, Y.; Yoshinari, N.; Naruse, D.; Nozaki, K.; Konno, T. *Inorg. Chem.* **2013**, *52*, 14368-14375. (b) Yoshinari, N.; Kakuya, A.; Lee, R.; Konno, T. *Bull. Chem. Soc. Jpn.* **2015**, *88*, 59-68.

(13) (a) Lee, R.; Igashira-Kamiyama, A.; Okumura, M.; Konno, T. *Bull. Chem. Soc. Jpn.* **2013**, *86*, 908-920. (b) Hashimoto, Y.; Yoshinari, N.; Matsushita, N.; Konno, T. *Eur. J. Inorg. Chem.* **2014**, 3474-3478. (c) Oji, K.; Igashira-Kamiyama, A.; Yoshinari, N.; Konno, T. *Angew. Chem. Int. Ed.* **2014**, *53*, 1992-1996.

(14) Lindner, E.; Fawzi, R.; Mayer, H. A.; Eichele, K.; Hiller, W. *Organometallics*, **1992**, *11*, 1033-1043.

(15) See the Supporting Information.

(16) Yoshinari, N.; Hashimoto, Y.; Igashira-Kamiyama, A.; Konno, T. *Bull. Chem. Soc. Jpn.* **2011**, *84*, 623-625.

(17) Nakamoto, K. *Infrared and Raman Spectra of Inorganic and Coordination Compounds*, 5th ed., Wiley, Chichester, 1997.

(18) Ronda, C. R. In *Luminescence from Theory to Applications*; Ronda, C. R., Ed.; Wiley-VCH Verlag: Weinheim, Germany, 2008; Chapter 1, pp 1-34.

(19) The number of solvated water molecules in **1b** and **2b** calculated from the elemental analysis ($3\text{H}_2\text{O}$) is lower than that calculated from the TG analysis (Figure S17)¹⁵ and found in X-ray structural analysis ($4\text{H}_2\text{O}$). This is most likely due to the partial loss of water molecules from the samples during the elemental analysis procedures.

(20) A non-emissive amorphous sample was formed when **1a** was stored in *vacuo*, indicating the loss of a long-range ordering of crystal by the loss of methanol molecules. When the non-emissive amorphous sample was exposed to methanol vapor, the yellow emission was recovered although the sample was still in an amorphous phase. This implies that the non-radiating process is inhibited by the presence of methanol molecules that form H-bonding and $\text{C-H}\cdots\pi$ interactions with complex molecules. The non-emissive amorphous sample was converted to **1b** when it was exposed to moist air.

(21) Each crystalline sample of **1b** after exposing acetone, CH_2Cl_2 , CH_3CN , benzene, or cyclohexane showed a weak PXRD, which is distinct from those of **1a**, **1b** and **1c** (Figure S18).¹⁵ This implies that the exposure of VOCs other than methanol also causes some structural transformation in the solid state.

(22) In the infrared (IR) spectra (Figure S2),¹⁵ **1a** showed a C=O stretching band at 1603 cm⁻¹, which is lower energy than those in **1b** (1606 cm⁻¹) and **1c** (1604 cm⁻¹). This is compatible with the stronger intermolecular COO-H₂N hydrogen bond in **1a**.

(23) Methanol molecule possesses both hydrophobic methyl and hydrophilic hydroxyl groups, which can form C-H... π and O-H...O H-bonding interactions with complex molecules. The capability to form these non-covalent interactions, as well as the appropriate molecular size for incorporating in the emissive crystalline phase in **1a**, would be main reasons for the high vapor selectivity of methanol molecules over other VOCs.

(24) Naka, K.; Kato, T.; Watase, S.; Matsukawa, K. *Inorg. Chem.* **2012**, *51*, 4420-4422.

(25) Rawashdeh-Omary, M. A.; Rashdan, M. D.; Dharanipathi, S.; Elbjeirami, O.; Ramesh, P.; Dias, H. V. R. *Chem. Commun.* **2011**, *47*, 1160-1162.

(26) Kobayashi, A.; Fukuzawa, Y.; Chang, H.-C.; Kato, M. *Inorg. Chem.* **2012**, *51*, 7508-7519.

(27) Housecroft, C. E.; Shaykh, B. A. M.; Rheingold, A. L.; Haggerty, B. S. *Inorg. Chem.* **1991**, *30*, 130-133.

(28) Evans, R. C.; Douglas, P.; Winscom, C. J. *Coord. Chem. Rev.* **2006**, *250*, 2093-2126.

(29) (a) Kuwabara, J.; Ogawa, Y.; Taketoshi, A.; Kanbara, T. *J. Organomet. Chem.* **2011**, *696*, 1289-1293. (b) Chow, P. K.; Ma, C.; To, W.-P.; Tong, G. S. M.; Lai, S.-L.; Kui, S. C. F.; Kwok, W.-M.; Che, C.-M. *Angew. Chem. Int. Ed.* **2013**, *52*, 11775-11779.

(30) Suzuki, K.; Kobayashi, A.; Kaneko, S.; Takehira, K.; Yoshihara, T.; Ishida, H.; Shiina, Y.; Oishi, S.; Tobita, S. *Phys. Chem. Chem. Phys.* **2009**, *11*, 9850-9860.

(31) Yutaka, T.; Obara, S.; Ogawa, S.; Nozaki, K.; Ikeda, N.; Ohno, T.; Ishii, Y.; Sakai, K.; Haga, M. *Inorg. Chem.* **2005**, *44*, 4737-4746.

(32) Sheldrick, G. M. *Acta Cryst.* **2008**, *A64*, 112-122.

(33) Gaussian 09, Revision A.02, M Frisch, M. J.; Trucks, G. W.; Schlegel, H. B.; Scuseria, G. E.; Robb, M. A.; Cheeseman, J. R.; Scalmani, G.; Barone, V.; Mennucci, B.; Petersson, G. A.; S93 Nakatsuji, H.; Caricato, M.; Li, X.; Hratchian, H. P.; Izmaylov, A. F.; Bloino, J.; Zheng, G.; Sonnenberg, J. L.; Hada, M.; Ehara, M.; Toyota, K.; Fukuda, R.; Hasegawa, J.; Ishida, M.; Nakajima, T.; Honda, Y.; Kitao, O.; Nakai, H.; Vreven, T.; Montgomery, J. A. Jr.; Peralta, J. E.; Ogliaro, F.; Bearpark, M.; Heyd, J. J.; Brothers, E.; Kudin, K. N.; Staroverov, V. N.; Kobayashi, R.; Normand, J.; Raghavachari, K.; Rendell, A.; Burant, J. C.; Iyengar, S. S.; Tomasi, J.; Cossi, M.; Rega, N.; Millam, J. M.; Klene, M.; Knox, J. E.; Cross, J. B.; Bakken, V.; Adamo, C.; Jaramillo, J.; Gomperts, R.; Stratmann, R. E.; Yazyev, O.; Austin, A. J.; Cammi, R.; Pomelli, C.; Ochterski, J. W.; Martin, R. L.; Morokuma, K.; Zakrzewski, V. G.; Voth, G. A.; Salvador, P.; Dannenberg, J. J.; Dapprich, S.; Daniels, A. D.; Farkas, O.; Foresman, J. B.; Ortiz, J. V.; Cioslowski, J.; Fox, D. J. Gaussian, Inc., Wallingford CT, 2009.

(34) (a) Becke, A. D. *J. Chem. Phys.* **1993**, *98*, 5648. (b) Becke, A. D. *Phys. Rev. A* **1988**, *38*, 3098. (c) Lee, C.; Yang, W.; Parr, R. G. *Phys. Rev. B* **1988**, *37*, 785.

(35) (a) Hay, P. J.; Wadt, W. R.; *J. Chem. Phys.* **1985**, *82*, 270. (b) Wadt, W. R.; Hay, P. J. *J. Chem. Phys.* **1985**, *82*, 284. (c) Hay, P. J.; Wadt, W. R. *J. Chem. Phys.* **1985**, *82*, 299.

Table 1. Diffuse reflection, excitation (ex), and emission (em) data in the solid state at room temperature.

compounds	reflection: $\lambda_{\text{max}}/\text{nm}$	ex: $\lambda_{\text{max}}/\text{nm}$	em: $\lambda_{\text{max}}/\text{nm}$	Φ	$\tau/\mu\text{s}$, (fraction)
[1] \cdot 1.5H ₂ O \cdot 1.5 CH ₃ OH (1a)	338	286, 315, 348	531	0.10	1.11
[1] \cdot 4H ₂ O (1b)				0.015	0.32(12%), 0.069(25%), 0.016(63%)
[2] \cdot 1.5H ₂ O \cdot 1.5 CH ₃ OH (2a)	418	352, 444	635	0.017	
[2] \cdot 4H ₂ O (2b)				<0.003	

Table 2. Crystal data of Complexes.

	[1]·1.5CH ₃ O H·1.5H ₂ O (1a)	[1]·7H ₂ O (1c)	[1]·4H ₂ O (1b)	[2]·1.5CH ₃ O H·1.5H ₂ O (2a)	[2]·7H ₂ O (2c)	[2]·4H ₂ O (2b)
empirical formula	C ₆₃ H ₇₄ N ₂ O ₁₀ P ₄ Pt ₂ S ₂	C ₁₂₀ H ₁₂₄ N ₄ O ₃₆ P ₈ Pt ₄ S ₄	C ₁₂₀ H ₁₂₄ N ₄ O ₂₄ P ₈ Pt ₄ S ₄	C ₆₃ H ₇₄ N ₂ O ₁₀ P ₈ P ₄ Pd ₂ S ₂	C ₁₂₀ H ₁₂₄ N ₄ O ₃₆ P ₈ Pd ₄ S ₄	C ₁₂₀ H ₁₂₄ N ₄ O ₂₄ P ₈ Pd ₄ S ₄
fw	1597.42	3354.58	3162.58	1420.04	2999.82	2807.82
size / mm ³	0.15 x 0.02 x 0.02	0.20 x 0.20 x 0.10	0.12 x 0.10 x 0.10	0.15 x 0.05 x 0.03	0.20 x 0.20 x 0.10	0.15 x 0.10 x 0.10
crystal system	Orthorhombic	Triclinic	Triclinic	Orthorhombic	Triclinic	Triclinic
space group	<i>P</i> 2 ₁ 2 ₁ 2 ₁	<i>P</i> 1	<i>P</i> 1	<i>P</i> 2 ₁ 2 ₁ 2 ₁	<i>P</i> 1	<i>P</i> 1
<i>a</i> / Å	13.0435(7)	13.0894(2)	13.352(2)	13.1259(2)	13.1073(8)	13.375(2)
<i>b</i> / Å	18.7020(10)	15.7129(3)	14.784(3)	18.8248(3)	15.7964(8)	14.699(3)
<i>c</i> / Å	27.3566(19)	19.3044(4)	19.314(4)	27.4833(5)	19.3997(8)	19.198(4)
α / °	90	79.510(6)	75.711(5)	90	79.292(6)	75.569(5)
β / °	90	70.921(5)	69.782(5)	90	71.117(5)	70.129(5)
γ / °	90	70.034(5)	65.683(5)	90	69.573(5)	65.587(5)
<i>V</i> / Å ³	6673.4(7)	3515.6(2)	3235.6(10)	6790.92(19)	3549.5(4)	3206.0(10)
<i>Z</i>	4	1	1	4	1	1
<i>T</i> / K	200(2)	200(2)	200(2)	200(2)	200(2)	200(2)
<i>R</i> (int)	0.0735	0.0189	0.0176	0.0290	0.0141	0.0137
ρ_{calcd} / g cm ⁻³	1.590	1.584	1.623	1.389	1.403	1.454
μ (Mo K α), mm ⁻¹	4.402	4.190	4.541	0.740	0.720	0.785
θ_{Max} / °	27.49	30.03	27.49	27.48	27.48	27.48
total no. of data	49579	40637	25632	54510	28711	25700
no. of unique data	15252	33304	22855	15525	25436	22901
no. of parameters	763	1445	1477	754	1445	1477
flack	0.026(4)	0.019(3)	0.008(4)	0.001(5)	−0.004(6)	0.000(9)
<i>R</i> (<i>I</i> > 2 σ (<i>I</i>)) ^a	0.0668	0.0324	0.0304	0.0433	0.0369	0.0322
<i>R</i> w ^b	0.1249	0.0908	0.0810	0.1140	0.1034	0.0827

a) $R1 = \Sigma||F_o| - |F_c|| / \Sigma|F_o|$.

b) $wR2 = [\Sigma(w(F_o^2 - F_c^2)^2) / \Sigma w(F_o^2)^2]^{1/2}$.

Figure 1. Molecular structure of [M(dppp)(L-cys)] (left). Interconversion among three different crystalline states; (i) stored in air, (ii) exposed to methanol vapor, (iii) recrystallized from a mixture of methanol/water (1:3), and (iv) stored in air (right).

Figure 2. (a) The perspective view of one of two independent complex molecules with 50% ellipsoids in **1a**. (b) Top and (c) side views of the left-handed four-fold helix. (d) CH– π interactions found around one methanol molecule. Dashed lines indicate hydrogen bonds.

Figure 3. (a) Diffuse reflection spectra of **1a** (red), **1b** (black), and **1c** (blue). (b) Excitation and emission spectra of **1a** ($\lambda_{\text{ex}} = 350$ nm, $\lambda_{\text{em}} = 530$ nm). (c) The change of emission spectra of **1a** in air. (d) The change of emission spectra of **1b** in methanol vapor. (e) A plot of the relative intensity of the emission of **1b** during repeated experiments of methanol exposure and storage in air. (f) Photographs of **1a**, (g) **1b**, (h) **2a**, (i) **2b** under UV light irradiation.

Figure 4. (a) The perspective view of one of four independent complex molecules with 50% ellipsoids and (b) a perspective view of the tetrameric structure in **1b**. (c) The perspective view of one of four independent complex molecules with 50% ellipsoids and (d) a perspective view of the dimeric structure in **1c**. Dashed lines indicate hydrogen bonds.

Figure 1

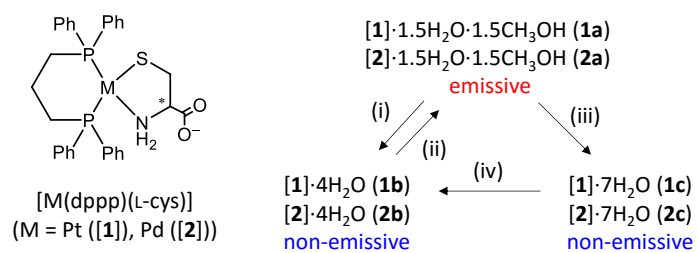


Figure 2

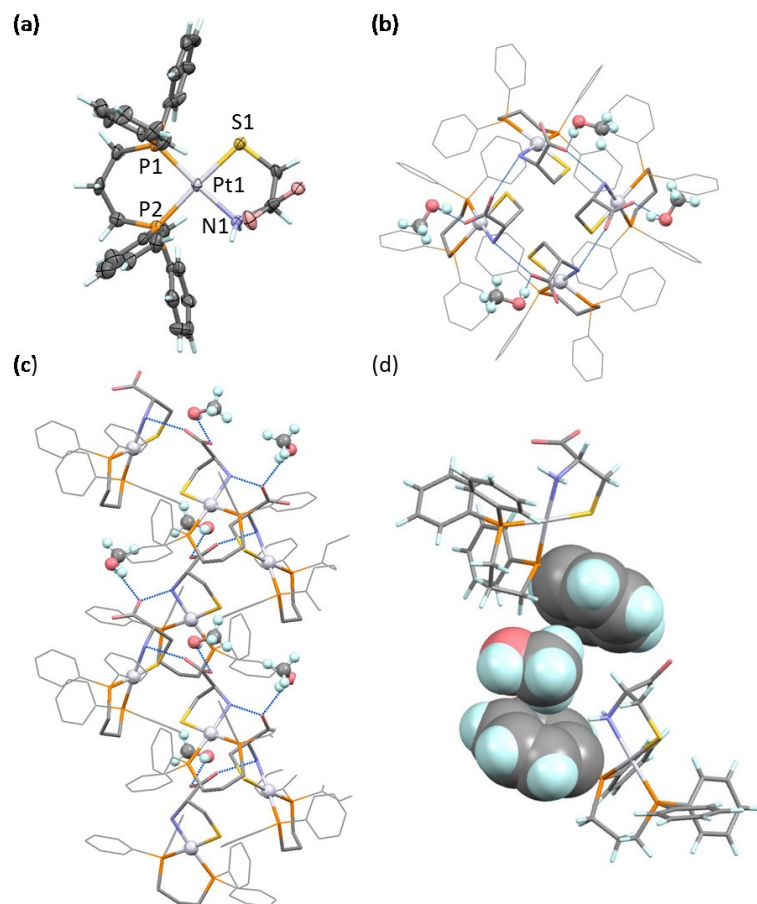


Figure 3

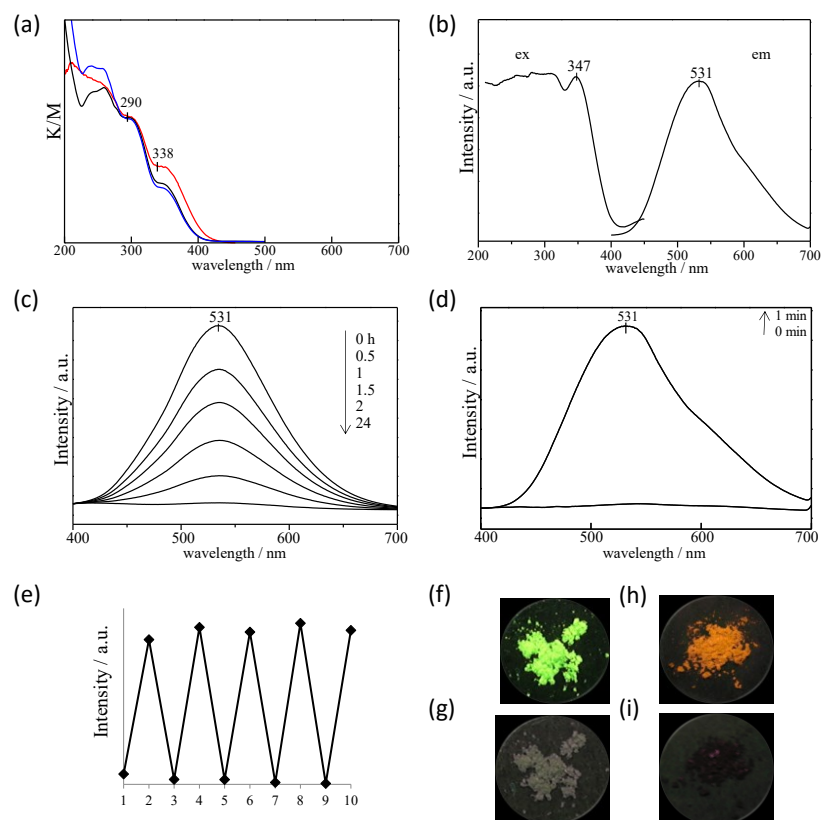
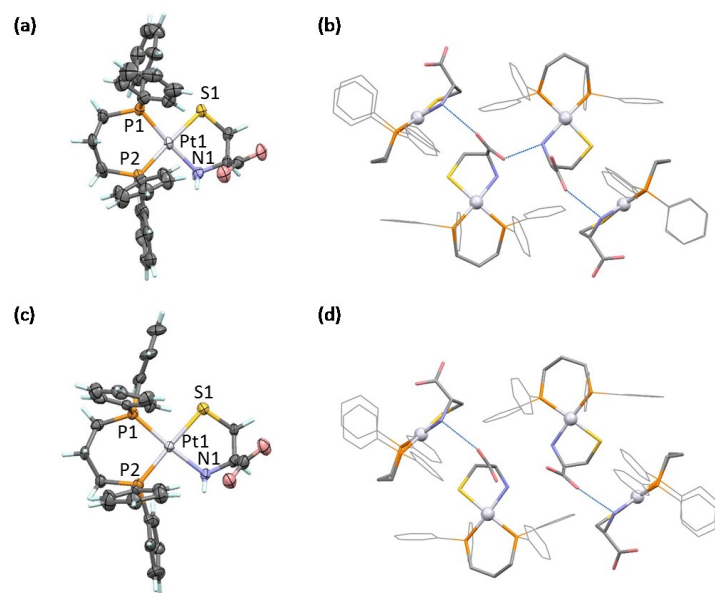
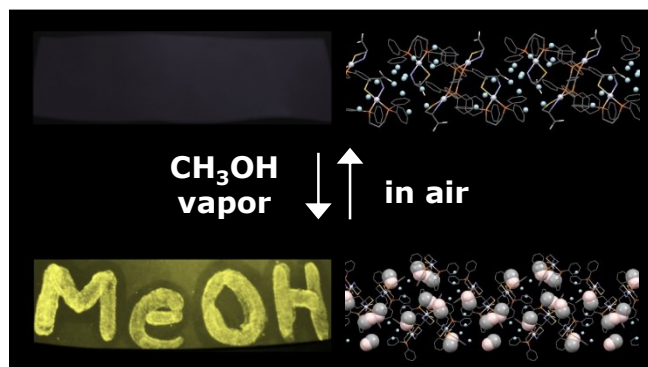


Figure 4



For Table of Contents Only



Square-planar palladium(II) and platinum(II) systems show reversible turn-on-type photoluminescence triggered by methanol vapor. Single-crystal X-ray crystallography revealed that methanol molecules form O-H \cdots O and CH \cdots π interactions with the complex molecules, which prevent vibrational emission quenching.